NeuroImage **12,** 184–195 (2000)
doi:10.1006/nimg.2000.0607, available online at http://www.idealibrary.com on IDEAL®

# Regularization of Diffusion-Based Direction Maps for the Tracking of Brain White Matter Fascicles

C. Poupon,*,† C. A. Clark,* V. Frouin,* J. Régis,‡ I. Bloch,† D. Le Bihan,* and J.-F. Mangin*

**Service Hospitalier Frédéric Joliot, CEA, 4 Place du Général Leclerc, 91401 Orsay Cedex, France; †Département Signal et Image, ENST, Paris, France; and ‡Service de Neurochirurgie Fonctionnelle et Stéréotaxique, CHU, La Timone, France*

Received November 2, 1999

**Magnetic resonance diffusion tensor imaging (DTI) provides information about fiber local directions in brain white matter. This paper addresses inference of the connectivity induced by fascicles made up of numerous fibers from such diffusion data. The usual fascicle tracking idea, which consists of following locally the direction of highest diffusion, is prone to erroneous forks because of problems induced by fiber crossing. In this paper, this difficulty is partly overcomed by the use of a priori knowledge of the low curvature of most of the fascicles. This knowledge is embedded in a model of the bending energy of a spaghetti plate representation of the white matter used to compute a regularized fascicle direction map. A new tracking algorithm is then proposed to highlight putative fascicle trajectories from this direction map. This algorithm takes into account potential fan shaped junctions between fascicles. A study of the tracking behavior according to the influence given to the a priori knowledge is proposed and concrete tracking results obtained with *in vivo* human brain data are illustrated. These results include putative trajectories of some pyramidal, commissural, and various association fibers.** © 2000 Academic Press

***Key Words:*** **diffusion; connectivity; white matter; fiber; regularization.**

## INTRODUCTION

The study of connectivity in the human brain is of interest to a wide range of investigators in the neuroscience community and encompasses fields of research concerned with the functional and anatomical organization of the brain, focal lesion-deficit studies, and brain development (Dejerine, 1895; Rye, 1999).

MRI is a unique tool for providing *in vivo* images of the brain for analysis of brain structure and organization. T1-weighted volume scans have been used to segment brain structures allowing automatic parcellation of the white matter and cortex (Filipek *et al.*, 1989; Mangin *et al.*, 1995; Meyer *et al.*, 1999; Makris *et al.*, 1999). These high-resolution MRI-based methods can be used to investigate the spatial relationships between anatomical regions. They are, however, unable to infer the connectivity induced by axonal fibers.

Tract tracing methodologies dedicated to the human brain have been restricted to post mortem studies. These methods include the dissection of white matter (Dejerine, 1895), strychnine neuronography (Pribam and MacLean, 1953), and the Nauta (Whitlock and Nauta, 1956) and Fink-Heimer methods (Turner *et al.*, 1980) of tracing neuronal degeneration after localized lesions. New histological methods have been recently proposed to study heavily myelinated fiber tracts in the normal brain (Bürgel *et al.*, 1999). Methods based on active axonal transport of tracer molecules, however, are restricted to animals for all but the shortest of pathways (Young *et al.*, 1995). These approaches which require animal sacrifice are limited by the number of injections (each of which may track only a few fiber bundles) in the same individual. *In vivo* MR imaging of the tracer could overcome this difficulty (Pautler *et al.*, 1998).

MRI methods based on the study of water diffusion in the human brain represent a promising new approach for fiber tracking and the study of connectivity. Diffusion imaging provides unique quantitative information about brain structure, which is completely noninvasive and covers the entire brain (see (LeBihan, 1991; Le Bihan, 1995) for a review). The basic principle stems from the orientational information provided by the phenomenon of diffusion anisotropy in white matter. Diffusion tensor imaging (DTI) characterizes the diffusional behavior of water in tissue on a pixel by pixel basis. This is done in terms of a matrix quantity from which the diffusion coefficient can be obtained corresponding to any direction in space (Basser *et al.*, 1994b). Subsequent diagonalization of the diffusion tensor yields its eigenvalues and eigenvectors. As such, the eigenvector corresponding to the largest eigenvalue is taken to represent the main direction of diffusion in a voxel. Given that one may ascribe diffusion anisotropy in white matter to a greater hindrance or restric-



1053-8119/00 $35.00

tion to diffusion across the fiber axes than along them, the principal eigenvector may be considered to point along the direction of a putative fiber bundle traversing the voxel. Thus direction maps made up of the principal eigenvectors can be produced, providing a striking visualization of the white matter pathways and their orientation (Makris *et al.*, 1997).

Several approaches have been recently proposed to study anatomical connectivity from such direction maps (Basser, 1998; Poupon *et al.*, 1998b, 1998a; Mori *et al.*, 1999; Conturo *et al.*, 1999; Xu *et al.*, 1999). The general aim is the possibility of asserting which cortical areas or basal ganglia are connected by fascicles embedded in white matter bundles. All these approaches rely on variants of the idea of locally following the direction of highest diffusion to reveal a fascicle trajectory. Unfortunately, *in vivo* protocols for diffusion image acquisition suffer from partial volume effect and various artifacts which lead to corrupted direction maps. For instance, as a result of partial volume, the direction of highest diffusion may not be related in a simple way to the underlying fascicle direction because of fiber crossing (Pierpaoli *et al.*, 1996a, 1996b; Tuch *et al.*, 1999). As each error in the direction map may lead to an erroneous fork for a local tracking process, this situation prevents robust fascicle tracking.

This paper proposes a new approach which consists of using *a priori* knowledge of white matter geometry to attempt to overcome such difficulties. The approach relies on a global model of the likelihood of any fascicle direction map. This model is used within a Bayesian framework to compute a regularized direction map allowing a global trade-off between diffusion tensor data and *a priori* knowledge regarding the low curvature of most of the fascicles. This regularized direction map is then used to perform tracking operations according to a new algorithm dealing with potential fan-shaped junctions between fascicles. Various results obtained in a series of normal volunteers show that the regularization approach improves the tracking robustness.

## METHODS

### *Data Acquisition*

All scans were acquired on a 1.5T Signa Horizon Echospeed MRI system (Signa, General Electric Medical Systems, Milwaukee, WI) equipped with magnetic field gradients of up to 22 mT/m. A standard quadrature head coil was used for RF transmission and reception of the NMR signal. Head motion was minimised with standard foam padding as provided by the manufacturer. The images were acquired after a sagittal localizer scan.

An inversion recovery prepared spoiled gradient echo sequence was used to obtain a volume image of the entire brain with a resolution of $256 \times 192 \times 124$ slice locations each 1.3 mm thick. The field of view = $24 \times 18$ cm along the read and phase directions respectively. Flip angle = 10°, $TE$ = 2.2 ms, $TI$ = 600 ms. Four excitations were acquired. Imaging time was approximately 27 min.

Echoplanar diffusion-weighted images were acquired in the axial plane. Blocks of eight contiguous slices were acquired each 2.8 mm thick. Seven blocks were acquired covering the entire brain corresponding to 56 slice locations. For each slice location 31 images were acquired; a T2-weighted image with no diffusion sensitisation followed by 5 diffusion sensitized sets ($b$ values linearly incremented to a maximum value of 1000 s/mm$^2$) in each of 6 noncolinear directions. These directions were as follows: {(1, 1, 0), (1, 0, 1), (0, 1, 1), (1, −1, 0), (1, 0, −1), (0, 1, −1)} providing the best precision in the tensor component when 6 directions are used (Pierpaoli *et al.*, 1996b).

In order to improve the signal to noise ratio this was repeated 4 times, providing 124 images per slice location. The image resolution was $128 \times 128$, field of view $24 \times 24$ cm, $TE$ = 84.4 ms, $TR$ = 2.5 s. Imaging time excluding time for on-line reconstruction was approximately 37 min. A database of 8 normal volunteers (men, age range 25–34 years) has been acquired with this protocol. All subjects gave informed consent and the study was approved by the local Ethic Committee.

### *Computation of the Diffusion Tensor*

Before performing the tensor estimation, an unwarping algorithm is applied to the diffusion-weighted dataset to correct for distortions related to eddy currents induced by the large diffusion sensitizing gradients. This algorithm relies on a three parameter distortion model including scale, shear, and linear translation in the phase-encoding direction (Haselgrove and Moore, 1996). The optimal parameters are assessed independently for each slice relative to the T2-weighted corresponding image by the maximization of an entropy-related similarity measure called mutual information (Wells III *et al.*, 1997). Following the distorsion correction, the diffusion tensor, and, subsequently, the eigen system are calculated for each voxel of the brain using a robust version of the method described in (Basser *et al.*, 1994a). This robust regression method is a $M$ estimator, which can be regarded as an iterated weighted least-squares (Meer *et al.*, 1991). This method remains reliable if less than half of the data are contaminated by outliers. A detailed description of this tensor reconstruction process is beyond the scope of this paper (Poupon, 1999b). The improvements induced by distortion correction and robust regression are illustrated by Fig. 1.

### *Direction Map Regularization*

*Ill-posed nature of the tracking problem.* Let us assume now that the fascicle tracking problem consists of

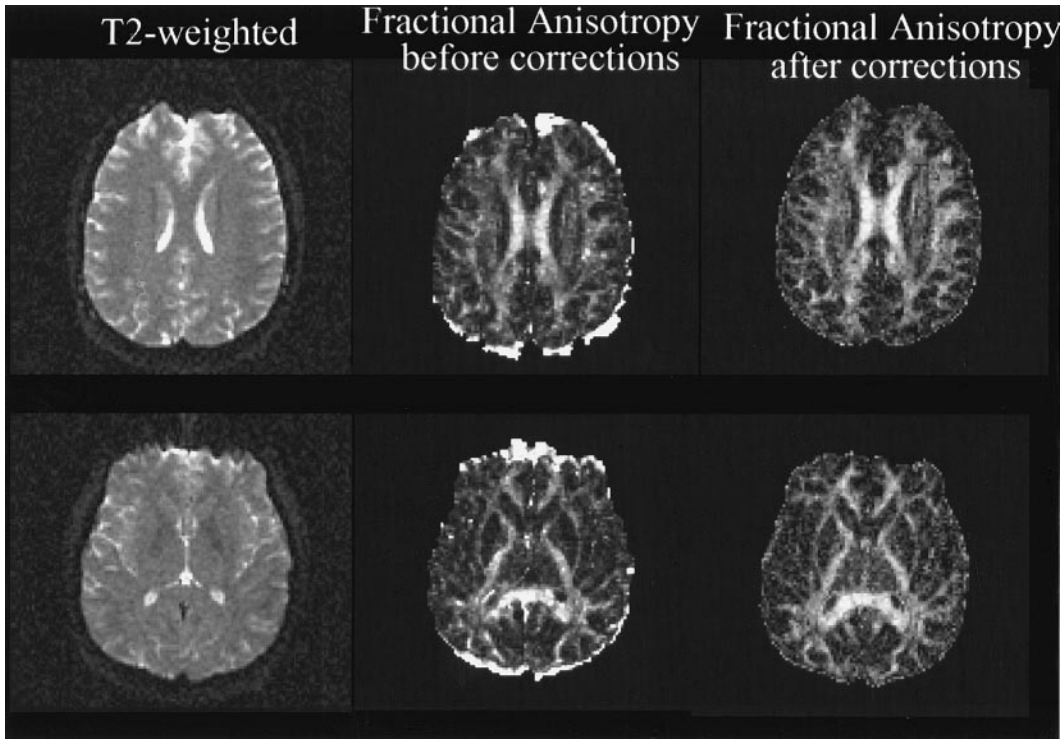


**FIG. 1.** Correction for the spatial distortions induced by eddy currents and computation of diffusion tensor using a robust regression method highly improves anisotropy maps. For instance, artifactual white areas induced by these distorsions in the phase-encoding direction have disappeared and the gray/white boundary is better defined.

inferring trajectories from a fascicle direction map extracted from tensor diffusion data. It should be noted that the spatial sampling of this direction map may be higher than the spatial resolution of diffusion data. This sampling may even be continuous when an interpolation method is used (Conturo *et al.*, 1999). Consequently, the fascicle tracking problem is very similar to a number of problems where "flow lines" have to be inferred from a vector field. The flow line running through a given location may be reconstructed bidirectionally by incremental displacements in the local vector direction. All the methods proposed to date follow this idea in conjunction with a stop criterion, which relies on thresholding tensor anisotropy (Conturo *et al.*, 1999) or trajectory curvature (Mori *et al.*, 1999).

While such flow line local reconstruction approaches may give very good results with a smooth vector field, stemming for instance from the simulation of some partial differential equation, they turn out to be questionable when applied to a corrupted vector field resulting from noisy observations. Indeed, it has to be understood that each erroneous vector may yield an erroneous fork of the trajectory reconstruction process. Hence, this local tracking method is unable to tolerate even one corrupted vector along a fascicle.

All the methods described up to now use the vector field made up of the tensor eigenvector related to the largest tensor eigenvalue. Unfortunately, this vector field is error prone. First, the low spatial resolution of diffusion weighted images with respect to the usual fiber bundle diameters encountered in the human brain leads to significant partial volume effects. If a voxel includes several fiber directions, the tensor is difficult to interpret. In such situations, the main eigenvector might follow a "mean direction" which may differ significantly from the directions of the underlying fascicles (Pierpaoli *et al.*, 1996a, 1996b; Tuch *et al.*, 1999). Furthermore, DTI is highly sensitive to physiological motion which may systematically lead to incorrect tensor estimation in some brain areas.

Considering that the corrupted nature of the eigenvector based direction maps is intrinsic to *in vivo* DTI of brain white matter, the tracking problem turns out to be "ill-posed." This mathematical terminology means here that two different DTI acquisitions of the same brain could lead to two highly different tracking results because of a high sensitivity to corrupted local directions. This type of situation, which is common in the field of computer vision, calls for the use of *a priori* knowledge on the tracking solution. Indeed *a priori* knowledge may allow the tracking algorithm to find the correct fascicle trajectory whatever the corrupted local directions.

*The regularized approach.* A vast amount of pathway specific knowledge could be used to constrain the

tracking algorithm. For instance some connections are known from post mortem studies and animal studies can be used to infer others. Furthermore, pathway diameter, dispersion, and anisotropy can be determined from previous studies. However, our current limited understanding of the variability of the human brain connectivity makes the use of such knowledge problematic (Bürgel *et al.*, 1999). Additionally, the use of such specific knowledge may prevent consistent studies of pathological brains. We have chosen therefore to use only a simple global assumption regarding the low curvature of most white matter fascicles. This kind of a priori knowledge leads to a classical paradigm of applied mathematics called regularization theory (Tikhonov and Arsenin, 1977).

The above introduction to the ill-posed nature of the fascicle tracking problem has led to two important observations. First, some principal eigenvectors do not follow the underlying fascicle directions. This will lead us to abandon the idea of using the tensor eigensystem to compute the direction map. Second, a local trajectory reconstruction is oblivious to corrupted vectors that produce erroneous forks. This will lead us to use a larger scale strategy in order to interpret ambiguous tensors.

Our new fascicle tracking method is made up of two stages. The first stage consists of computing a regularized fascicle direction map as the optimal trade-off between diffusion data and the low curvature hypothesis. For instance, while the direction of the first eigenvector of a "flat tensor" may largely differ from actual fiber directions, the plane defined from the first two eigenvectors is supposed to include these directions. Hence, the low curvature hypothesis will lead the regularization algorithm to choose within this plane the fascicle direction which provides the best agreement with the surrounding trajectories (see Fig. 2). The second stage of our method consists of studying brain connectivity using a simple tracking algorithm applied to this regularized direction map. Since this map is supposed to be error free, this algorithm relies on local information.

The initial step of our method consists of defining a mask $W$ within which all the algorithms are restricted. A first volume of interest made up of the voxels belonging to white matter is automatically extracted from the T1-weighted image using an algorithm developed in our institution (Mangin *et al.*, 1995, 1998). A sophisticated morphological dilation is then applied to this segmentation in order to be robust to potential distortions occuring in relating the echo-planar images (DTI) and the high resolution T1-weighted image mask. This dilation is homotopic which means that the topology of white matter is preserved (Mangin *et al.*, 1995) thus preventing the creation of impossible pathways through cortical folds.

The inference of the regularized direction map stems from a classical Bayesian interpretation. The regularized map $V_{opt}$ is the optimal map which maximizes the a posteriori probability $p(V|D)$, where $D$ denotes the diffusion tensor data set and $V$ denotes a random vector field which covers all possible direction maps defined on $W$. Bayes rule allows us to introduce the *a priori* knowledge on the low curvature of fascicles:

$$p(V|D) = \frac{p(D|V)p(V)}{p(D)}. \quad (1)$$

Since $p(D)$ does not depend on $V$, maximizing $p(V|D)$ amounts to maximizing the product $p(D|V)p(V)$. In the following, we propose a model of these two probabilities which allows the computation of $V_{opt}$. The *a priori* probability $p(V)$ will favor the direction maps made up of low curvature fascicles. The probability $p(D|V)$ will be related to the nature of water diffusion in white matter: for each voxel $M$, the diffusion coefficient in the direction $\vec{v}(M)$ should be as high as possible. Hence, the optimal map will be the best trade-off between the observations (the diffusion data) and the *a priori* knowledge (the low curvature assumption). An important point to be noted is that if $p(V)$ is the uniform probability density (no *a priori* knowledge), $V_{opt}$ turns out to be the usual map made up of the tensor principal eigenvectors.

*The spaghetti plate model.* Let us consider any direction map $V$ and a voxel $M$ of this map. According to this map, $\vec{v}(M)$ corresponds to the local direction of an underlying fascicle crossing voxel $M$. Assume now that we can find a way to compute the local curvature of this fascicle from the neighborhood of $M$ in the map. This can be achieved using local geometric relationships. Because fascicle curvature is the only information used to assess the likelihood of any direction map (without diffusion observations), then $p(\vec{v}(M))$ depends only on the realizations of the random vector field in the neighborhood of $M$. Random fields endowed with this property are called Markov fields. These fields have been intensively studied in statistical physics as models of spin glasses. Such fields are very interesting from a practical point of view because the global field probability $p(V)$ follows a Gibbs distribution (Geman and Geman, 1984):

$$p(V) = \frac{1}{Z} e^{-\Sigma_c P_c(V)}, \quad (2)$$

where $Z$ is a normalizing constant and $P_c$ are potential functions defined on subsets of neighboring points which interact with each other. These subsets are called cliques. Each clique $c$ possesses a potential function $P_c$, which embeds the nature of the local interaction. Intuitively, the lower the potential, the higher the

probability of the clique realization. It should be noted that one random variable (or one point) usually belongs to several cliques. Combining all potential functions leads to the global energy of the field, which is minimal for the most likely realizations, i.e., those having the highest probability.

We have recently introduced a class of Markovian models dedicated to direction map regularization (Poupon *et al.*, 1998a). In this paper, we focus on one specific model of this class which appears especially suitable to the tracking problem and stems from an intuitive analogy. At the resolution of our diffusion data, a lot of white matter voxels include some *trans*-callosal, some projectional, and some associational fibers (Dejerine, 1895). As a first approximation, however, the geometry of white matter may be compared with the geometry of spaghetti plates illustrated by Fig. 3. While this analogy will be used to describe our methodology, one has to bear in mind that this point of view is a significative simplification of the actual white matter geometry. Indeed, the striking simplicity of Fig. 3 dissection results in part from the fact that the anatomist was a talented sculptor who has discarded finer fascicles and fan-shaped endings.

**FIG. 3.** The spaghetti plate like geometry of white matter illustrated by a brain dissection (Williams *et al.*, 1997). The preservation method of Klinger was utilized. Fine forceps (straight or curved) were used to dissect the delicate nerve bundle preparations.

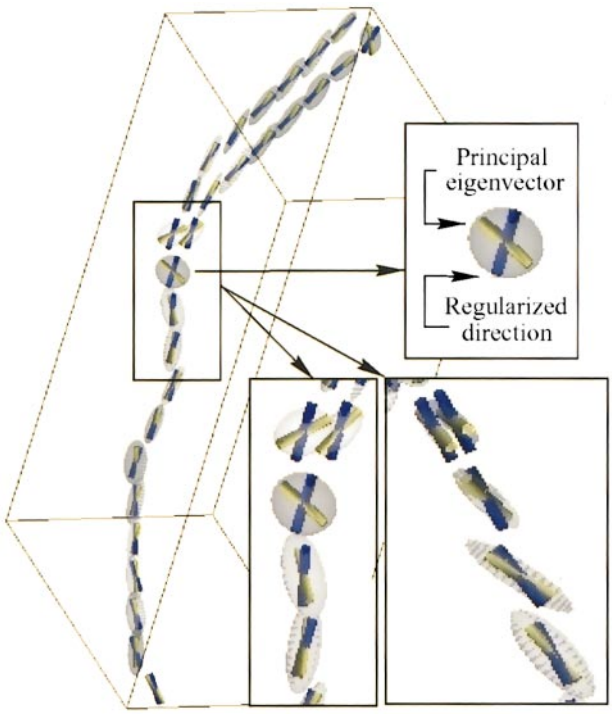


**FIG. 2.** The regularization idea illustrated by a Y shaped trajectory extracted from the pyramidal pathway. The diffusion tensors are represented by ellipsoids, the tensor principal eigenvectors by light yellow cylinders, and the regularized fascicle directions by dark blue cylinders. The trajectory has been obtained using a local tracking algorithm applied to the regularized direction map. This trajectory includes some flat tensors at the level of the Y junction. The principal eigenvectors of these flat tensors give low confidence information on actual fascicle directions. Therefore, a local tracking algorithm applied to the eigenvector map may lead to erroneous forks at the level of these flat tensors. The regularization algorithm has reoriented the putative fascicle directions in order to create low curvature trajectories while keeping a high diffusion coefficient along these directions. The largest corrections occur for the low anisotropy tensors.

Let us consider a single strand of spaghetti. Before any cooking, this spaghetti can be considered as a straight line. Put in hot water, the spaghetti accumulates some energy and becomes a bended curve. The magnitude of the total curvature is related to the total amount of energy which has been accumulated. A simple way to assess the cooking effect on the spaghetti geometry consists of integrating the curvature to derive the spaghetti bending energy $E$:

$$E(\text{spaghetti}) = \int_0^{\text{length}} \alpha c^2(s) ds; \qquad (3)$$

where $s$ is simply a curvilinear length measured along the spaghetti, $c(s)$ is the spaghetti curvature at distance $s$ from the origin and $\alpha$ is the spaghetti rigidity. This energy, well known in chemistry as the Kratky-Porod model of semi-flexible polymers (Chaikin and Lubensky, 1995), can be extended in a straightforward way to the whole spaghetti plate. Note now that the spaghetti energy defined in Eq. (3) breaks down to a sum of local terms related to the local curvature, which are exactly the kind of local interactions we are seeking to define a Gibbs distribution for the fascicle direction maps. Hence, the low curvature hypothesis will be translated into a low bending energy constraint.

It is still necessary, however, to design the way to compute the fascicle local bending energy. Let us return to the fascicle going through voxel $M$. Since fascicles cannot end inside white matter, we must find two

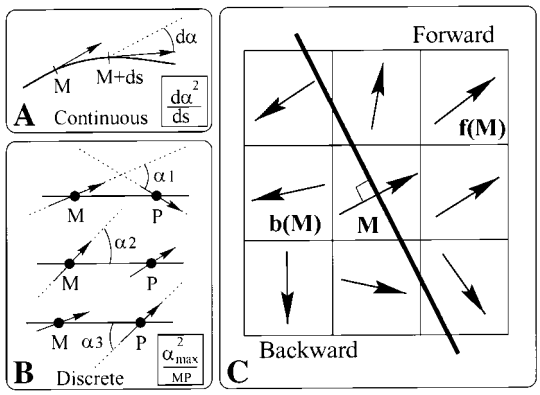


**FIG. 4.** 2-D illustration of the computation of fascicle local bending energy. (A) The spaghetti local bending energy. Note that $c^2 ds = (d\alpha/ds)^2 ds = d\alpha^2/ds$, where $c$ denotes local curvature (cf. Eq. 3). (B) A discrete bending energy is defined between two neighboring points in order to mimic the continuous case (cf. Eq. 4). (C) The 26-neighborhood of each point $M$ is split in two by a plane orthogonal to $\vec{v}(M)$ which defines forward and backward neighbors. One point minimizing the discrete bending energy is selected in each of these half-neighborhoods (forwards: $f(M)$, backwards: $b(M)$). The underlying fascicle is supposed to follow the $f(M) - M - b(M)$ trajectory.

prolonging voxels or perhaps the boundary of white matter. To be consistent with the spaghetti plate analogy, these linked voxels are defined from a criterion $e(M, P)$, which mimics the spaghetti local bending energy (see Fig. 4):

$$e(M,P) = \frac{\mathbf{max}^2((\vec{v}(M),\ \vec{u}_{MP}),\ (\vec{v}(P),\ \vec{u}_{MP}),\ (\vec{v}(M),\ \vec{v}(P)))}{\|\vec{MP}\|}, \tag{4}$$

where $\vec{u}_{MP} = \vec{MP}/\|\vec{MP}\|$ and $(\vec{u},\ \vec{v})$ denotes the angle between directions $\vec{u}$ and $\vec{v}$. The neighborhood of $M$ is split in two by a plane that defines forward and backward neighbors. Then one point minimizing $e(M, P)$ is selected in each of these half-neighborhoods (forward: $f(M)$, backward: $b(M)$). The underlying fascicle is supposed to follow the $f(M) - M - b(M)$ trajectory. The potentials used to define the Gibbs distribution follow directly:

$$P_M^S(V) = e(M, f(M)) + e(M, b(M)). \tag{5}$$

Because of the definitions of $f(M)$ and $b(M)$, the clique related to $P_M^S$ is the 26-neighborhood of $M$ (more precisely the points of the 26-neighborhood of $M$ included in $W$). The Gibbs distribution made up of these potentials gives a high probability to the direction maps endowed with a low global bending energy. Because of the analogy introduced above, this model is called later the spaghetti plate model. It should be noted that although this model is made up of local potentials, the probability distribution $p(V)$ is global. This endows our tracking model with a non local field of view.

*The diffusion information.* A model will now be proposed for the second probability $p(D|V)$. It should be noted by a reader unfamiliar with the Bayesian framework that $V$ is now fixed and supposed to represent an actual fascicle direction map. Let us assume that the tensor measurement in one voxel $M$ depends only on the local fascicle direction given by $\vec{v}(M)$. This reasonable hypothesis will lead to a second Gibbs distribution corresponding to a field without interaction. The probability $p(D|V)$ can be rewritten in the following way:

$$p(D|V) = \prod_M p(D(M)|\vec{v}(M)).$$

Assuming now that any tensor measurement $D(M)$ has a non-zero probability, $p(D|V)$ can be rewritten as:

$$p(D|V) = \frac{1}{Z^D} \prod_M e^{-P_M^D(\vec{v}(M))} = \frac{1}{Z^D} e^{-\Sigma_M P_M^D(\vec{v}(M))},$$

where $Z^D$ is a normalizing constant and $P_M^D(\vec{v}(M)) = -\ln(p(D(M)|\vec{v}(M)))$. Finally, in order to get a probability $p(D(M)|\vec{v}(M))$ decreasing with the discrepancy between diffusion in the direction $\vec{v}(M)$ and the largest diffusion coefficient $\lambda_1$ (the largest tensor eigenvalue), we propose the following potential function:

$$P_M^D(\vec{v}(M)) = \left(\frac{\vec{v}(M)\,{}^t D(M)\vec{v}(M) - \lambda_1}{\|D(M)\|}\right)^2. \tag{6}$$

The discrepancy is normalized by the tensor norm (Basser and Pierpaoli, 1996) in order to remove all diffusion-based information apart from anisotropy. For highly anisotropic tensors, this potential acts like a spring which tries to align $\vec{v}(M)$ along the direction of the largest diffusion coefficient. In the case of flat tensors, this potential is more flexible and allows $\vec{v}(M)$ to turn in the high diffusion plane. Finally, for isotropic tensors, this potential allows any fascicle direction.

*The entire model.* Combining all the previous equations leads to an expression for $p(V|D)$ which turns out to be a new Gibbs distribution:

$$p(V|D) = \frac{1}{Z} e^{-\Sigma_M P_M^D(\vec{v}(M)) + \alpha P_M^S(V)}, \tag{7}$$

where $Z$ is a normalizing constant. This new distribution now leads to the definition of $V_{\text{opt}}$ as the direction map that minimizes the energy given by:

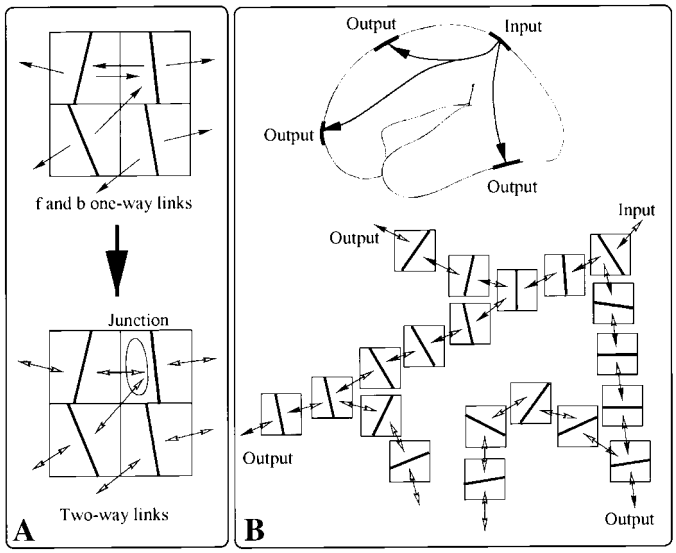


**FIG. 5.** The tracking system. (A) The regularized direction map is endowed with a system of two-way links. Some of the voxels which have more than one two-way link in the same half neighborhood turn out to be fascicle junctions. (B) The user selects one area on the white matter surface. Then a propagation algorithm follows the links until other white matter surface areas are reached. If the propagation comes across a junction voxel, several trajectories may be followed in parallel. The rule that prevents the propagation from proceeding backwards at junction voxels is simple: when a voxel is reached, the voxel mid-plan has to be crossed before using a new link. Black arrows indicate the links used in the example.

$$E(V) = \sum_M P_M^D(\vec{v}(M)) + \alpha \sum_M P_M^S(V). \qquad (8)$$

Finally, this last definition shows that the optimal direction map $V_{opt}$ is a trade-off between the measured tensor data and the a priori knowledge on the low curvature of fascicles. The constant $\alpha$ reflects the influence of this *a priori* knowledge, which is equivalent to the rigidity of the underlying spaghetti plate. Hence, $V_{opt}$ represents the low energy spaghetti plate with the highest diffusion along each spaghetti.

### *Tracking Experiments*

Once the regularized fascicle direction map $V_{opt}$ has been computed from the minimization of $E(V)$, the system user can perform tracking experiments according to a simple local tracking scheme. This scheme relies on the following organization of the direction map. Each $M - f(M)$ and $M - b(M)$ link defined according to the principle used during the regularization stage (see Fig. 4) is converted into a two-way link (see Fig. 5A). Recall that each voxel is endowed with forward and backward half-neighborhoods (see Fig. 4C). After the conversion operation, some of the voxels have more than one two-way link in the same half-neighborhood. These voxels prove to be junctions related either to fan-shaped divergences (see Fig. 2) or to variations of a bundle thickness.

The system user first selects one area on the white matter surface. Next a real-time propagation algorithm follows the two-way links until other areas of the white matter surface are reached (see Fig. 5B). Several areas may be reached if the propagation encounters junction voxels. Other kinds of experiments may also be performed. For example, the input area may be located inside white matter ($W$), in which case the propagation algorithm is bidirectional. Or two input areas, defined for instance by functional activations, may be specified. In this case the system performs the propagation from the first area and yields only the trajectories reaching the second area.

## RESULTS

For all the following results, the state space of the random vectors $\vec{v}(M)$ has been discretized in 162 uniformly distributed directions. A deterministic minimization algorithm has been used to find the local minimum for $E(V)$ the nearest to the principal eigenvector map (Besag, 1986). The computation time is about one hour on a conventional workstation. The resulting fascicle direction map is used to perform the tracking experiments.

### *Influence of the a Priori Model Weight*

Regularization of one set of diffusion tensor data has been performed with eleven different values of the weighting parameter $\alpha$ (the spaghetti rigidity). In order to then study the influence of regularization on the fascicle direction map geometry, the voxels have been classified into four types according to topological considerations. In order to assess the number of voxels leading to high local curvature trajectories, a threshold on the local bending energy has been used to remove some links. Since we will only focus on the evolution of the number of the created "dead ends" relative to $\alpha$, this threshold has been arbitrarily fixed to remove links leading to angular variations of more than 45 degree (see Fig. 4). The four types are:

*Simple fascicle nodes.* Voxels having exactly one two-way link in each half neighborhood;

*Junctions.* Voxels related to the merge (or split) of several fascicles made up of points of the previous type;

*Gate to gray matter.* Voxels leading to outside of the white matter.

*Dead ends.* Voxels without a link in one half-neighborhood.

Figure 6 presents the evolution from no regularization (left asymptotes) to high regularization (right). First, the number of pathological sites (see Fig. 6.3) decreases dramatically with the regularization which demonstrates the efficiency of the model.

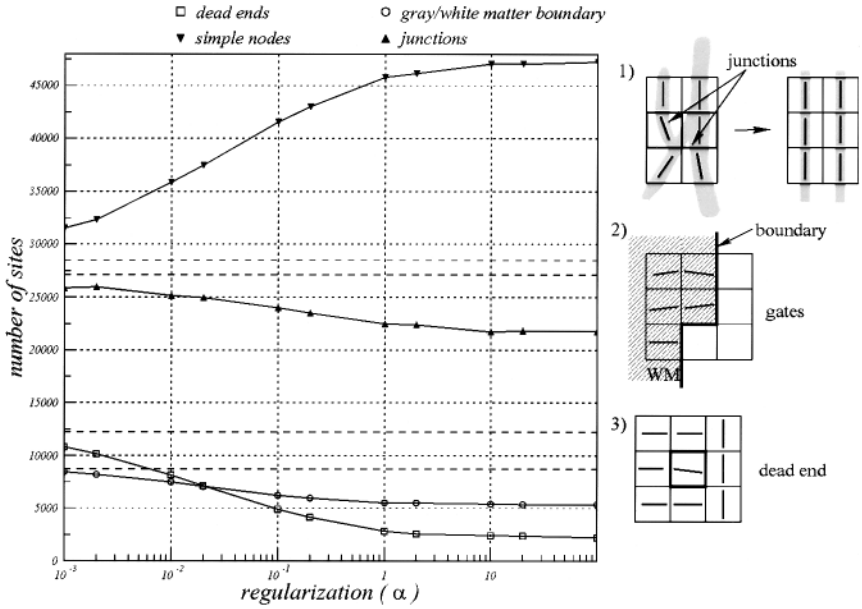


**FIG. 6.** (Left) Evolution of the numbers of four different types of configurations (see text); (right) (1) fascicle mixing inside a bundle before regularization versus parallel fascicles after regularization; (2) sites of white matter leading to gray matter; (3) dead end without tracking possibility.

Second, the regularization leads to a decreased number of junctions and to a dramatic increase in the number of simple fascicle nodes. This effect is mainly due to a reorganization of the fascicles inside larger bundles (see Fig. 6.1) which corresponds to the usual underlying anatomical reality. Indeed, the chronotopic establishment of the connections leads to topographically ordered bundles (Molnár, 1998). Hence, the large bundles develop somatotopic organizations, which means that different parts of the bundle section include axons connecting different brain areas. Some very long chains of simple fascicle nodes can be found inside large bundles (see Fig. 7). Finally, the number of sites leading to gray matter decreases slightly, which is related to the fact that our model prevents concave areas of the boundary, namely cortical fold bottoms, from straying outside the white matter. While this may correspond to some actual anatomical constraint, this observation calls for refinements of the regularizing model. All the curve evolutions reach limits beyond which no more topological effect is observed. This observation suggests that the weight $\alpha = 1$ is a reasonable trade-off between regularization and fidelity to the data which has been used for further experiments.

Apart from the topological experiments mentioned above, several experiments have been done to verify visually that the weight $\alpha = 1$ was not too high. These experiments have shown that the more important effects of regularization occur for voxels endowed with a low anisotropy (see Fig. 2).

*Tracking Experiments*

Finally, various tracking experiments have been performed according to the scheme proposed in Fig. 5 or to a similar one for which the input is located inside white matter. Some of these experiments were aimed at tracking the putative trajectories of short and long association fibers (cf. Figs. 8 and 9). Other experiments were aimed at tracking the putative trajectories of commissural fibers (cf. Fig. 10). Most of these experiments led to low curvature trajectories in accordance with the *a priori* knowledge used in the regularization process. The vast majority of these trajectories were given fan shaped terminations and a few forks compatible with the actual organization of white matter. While no real validation is currently available, some of these tracking experiments revealed trajectories akin to well-known white matter bundles described in the anatomical literature (Dejerine, 1895): pyramidal tracts (cf. Fig. 7), superior longitudinal fasciculus (cf. Fig. 8A), cingulum bundle (cf. Figs. 9A and 9B), occipito-frontal fasciculus (cf. Fig. 9C), occipito-occipital commissural axons crossing corpus callosum splenium (cf. Fig. 10). Tracking experiments stemming from inputs located in the corpus callosum show that it is possible to reveal a certain level of the somatotopic organization of this major commissure, even if the respective cortical areas reached from very close inputs may not be fully distinct (cf. red and green tracking from corpus callosum splenium in Fig. 10).

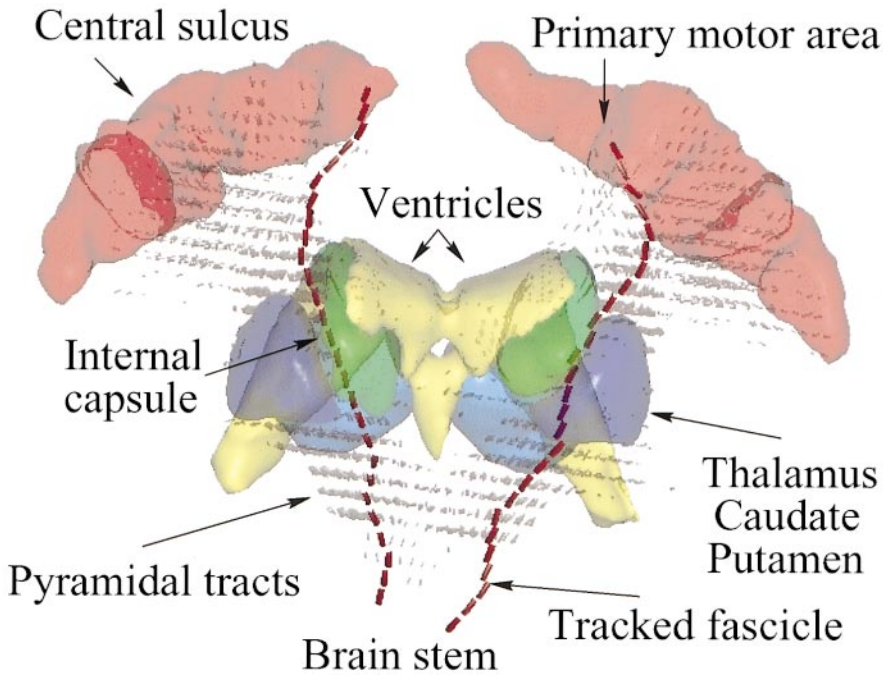


**FIG. 7.** Two sample elementary fascicles (made up of simple nodes) among the longest ones. The underlying pyramidal tracts have been defined using a connectivity based idea similar to the one proposed in (Jones *et al.*, 1999). The putative fiber orientation is indicated by cylinders.

## DISCUSSION

Recent *in vivo* studies of the rat brain using research MRI systems and long acquisition times have shown the feasibility of accessing brain connectivity using DTI (Xu *et al.*, 1999). Reaching similar results for the living human brain with clinical scanners and reasonable acquisition times remains a difficult challenge (Poupon *et al.*, 1998a; Conturo *et al.*, 1999). Fascicle tracking itself is a mathematically ill-posed problem especially sensitive to corrupted local directions in the map inferred from the DTI data. Each error in this direction map may lead to an erroneous fork of a local tracking process. This weakness is especially troublesome considering the problems induced by partial volume effects which mix fascicle directions. While partial volume effects may be decreased using higher spatial resolution, this solution reduces SNR and generally leads to more severe image artefacts. Fur-

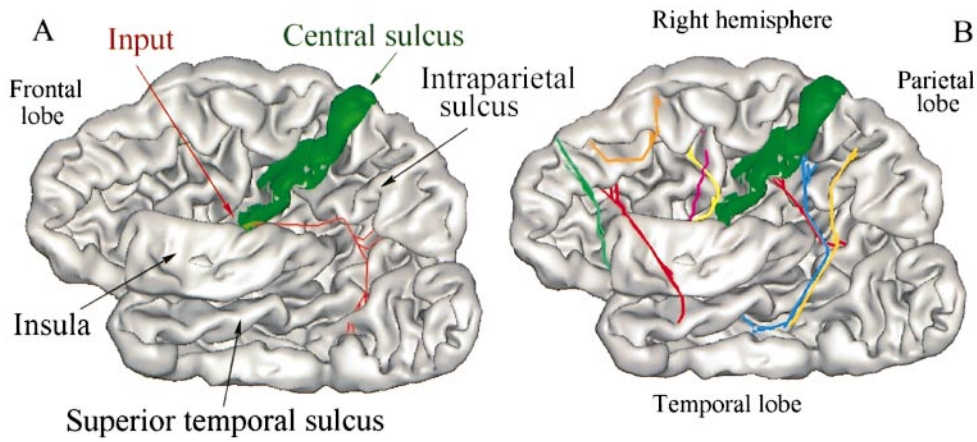


**FIG. 8.** Examples of tracking from one single input voxel. The right hemisphere cortex is visualised from inside after a virtual split into two pieces. (A) Input located in a premotor area leading to a long trajectory inside the superior longitudinal fasciculus including several forks towards inferior parietal lobule and temporal lobe. (B) Tracking from different white matter voxels highlights putative trajectories of short and long association fibers.

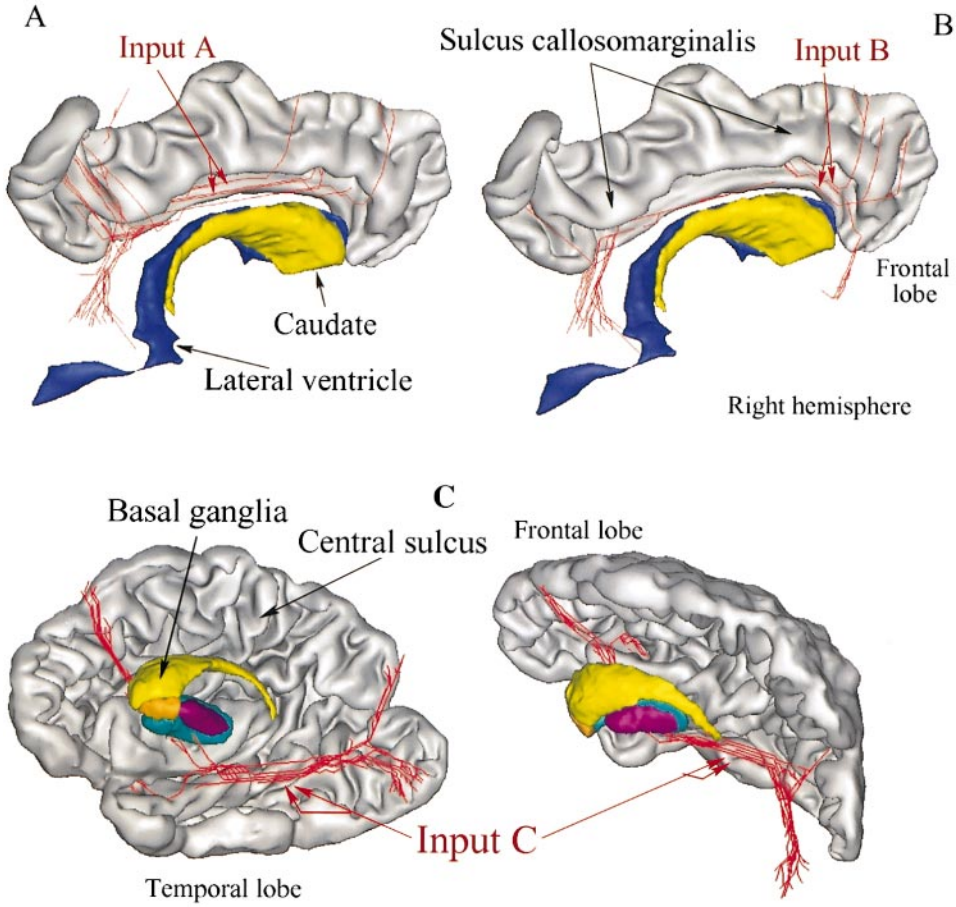


**FIG. 9.** Examples of tracking from small sets of neighboring voxels endowed with similar putative fiber orientations (as observed in 2-D slices with super-imposed directions). Input areas A and B are located inside right hemisphere cingulum bundle. Tracking highlights different parts of the underlying bundle with some branching towards other cortical areas. Input area C is located inside right temporal white matter. Tracking highlights the putative trajectory of the occipitofrontal fasciculus.

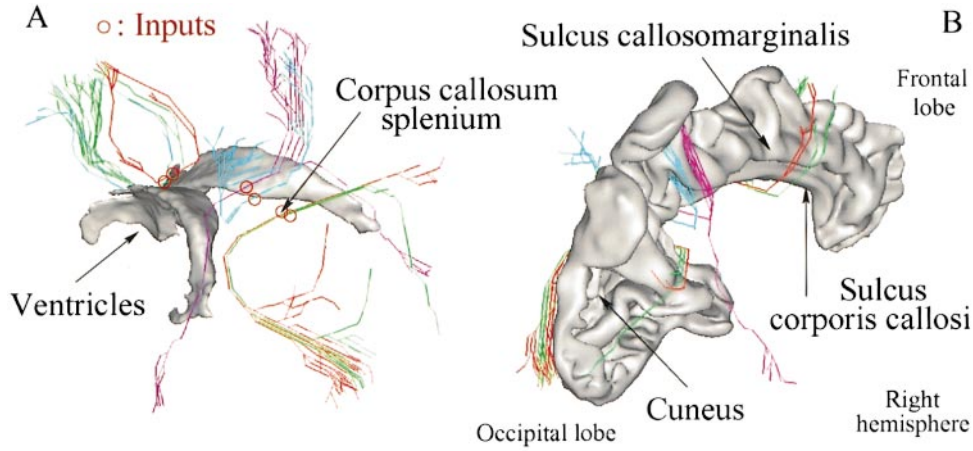


**FIG. 10.** Tracking from different voxels located in corpus callosum. The lateral ventricles (A) and a part of the right hemisphere cortex (B) are included in the visualizations for a better understanding of the trajectories.

thermore, considering the actual intercalated fine-grained anatomy of white matter, DTI cannot completely overcome partial volume effects without addressing finer diffusion models (Tuch *et al.*, 1999).

While high angular resolution diffusion models have to be used to untangle thin association bundles, we have shown in this paper that another promising direction of research consists of using *a priori* knowledge on the tracking solution. While the regularization method proposed in this paper may appear complicated compared to more usual image smoothing approaches, it should be noted that the underlying idea is a restoration that preserves the DTI spatial resolution. Considering the current spatial resolution of *in vivo* DTI (2 mm), preserving this resolution is crucial for the tracking of thin cortico-cortical bundles, which are of high interest in neuroscience. For instance, Gaussian smoothing of the tensor data, which has been recently proposed as a preprocessing to tracking (Westin *et al.*, 1999), is bound to increase partial volume effects. In return, our approach based on the fascicle low curvature hypothesis, can deal with some simple problems induced by partial volume effects (see Fig. 2). Our hypothesis, however, like a number of a priori knowledge, may be wrong in some situations. Nevertheless, since our approach is based on a trade-off between *a priori* knowledge and observations, actual fascicles endowed locally with high bending can be tracked when the underlying diffusion data is straightforward (highly anisotropic).

In a recent paper, Conturo *et al.* presented similar tracking results obtained for the living human brain (Conturo *et al.*, 1999). Their tracking approach and the one described in this paper differ on many points, however. First, Conturo *et al.* ask connectivity questions of a closed nature: which diffusion tracks cross these two specific regions of interest? This kind of question includes more constraints than open questions such as: which diffusion tracks cross this specific gray or white matter area? Imposing several localization constraints is an interesting way of dealing with the ill-posed nature of the tracking problem. Nevertheless, more open questions are required to explore brain connectivity. Moreover, it has to be noted that the user of the Conturo *et al.* method will have to decide whether he discards unplausible diffusion trajectories or he takes every result at face value. Hence, a second important difference is that the Conturo *et al.* method uses no *a priori* knowledge at all on the diffusion track geometry. In our opinion, such constraints are required not only to discard erroneous forks but also to recover some of the actual trajectories masked by partial volume and other artefacts (see Fig. 2).

A third difference between both tracking approaches is related to the interpolation of diffusion data used by Conturo *et al.* This interpolation allows the tracking process to get rid of potential bias induced by the discrete grid. An important issue which has to be answered is whether this interpolation results in an increase in the number of false forks followed by the tracking process. Indeed, interpolation is bound to create partial volume like direction mixing. A last difference is that our method deals explicitly with the fan shaped organization of fiber bundles while the Conturo *et al.* method relies on diffusion track oversampling. Their method cannot apparently account for fiber branching.

In another recent paper, Jones *et al.* proposed a voxel linking rule to define major bundles as connected components (Jones *et al.*, 1999). While this rule shares striking similarities with the tracking method described in our paper, it is too tolerant to deal with brain connectivity. Indeed, a bunch of bundles that cross the same white matter bottleneck (corpus callosum, internal capsule) belong to the same connected component because voxels of parallel bundles are often linked. In fact the notion of trajectory is missing in Jones *et al.* method. In return, the notion of best neighbors used in our paper leads to trajectories which allows us to split large bundles into fascicle sets.

A number of questions related to some of the parameters of our method remain open: the weight of a priori knowledge, the choice of the potential functions, the minimization algorithm. Furthermore, some refinements are required to overcome some bias induced by the discrete grid. Finally, our model of white matter should be improved in order to take fiber crossing into account. Indeed, our work with a priori knowledge is only a first attempt and should lead to further developments. Improving our general methodology will require knowledge of a gold standard with which to test the validity and accuracy of all refinements. One of the challenges to be immediately pursued, therefore, is the design of reliable validation approaches, using, for instance animals and standard tracer-based methods.

In summary, we have introduced a sequence of robust algorithms allowing the tracking of white matter fascicles using DTI. A number of these algorithms are completely new: eddy current distortion correction using mutual information, robust regression to assess the diffusion tensor, computation of a regularized direction map from DTI data and finally, a fascicle tracking algorithm dealing with fascicle junctions. An important future direction of research involves combining our regularization approach with diffusion data endowed with high angular resolution in order to deal with fascicles crossing inside a voxel (Tuch *et al.*, 1999). DTI based tracking methodologies yield for the first time access to the living human brain connectivity which may rapidly open numerous fields of appealing applications (Di Virgilio and Clarke, 1997; Rye, 1999).

## ACKNOWLEDGMENT

The authors are very grateful to Jonathan Oakley for his careful reading and useful comments on this manuscript.

## REFERENCES


Basser, P., Mattiello, J., and LeBihan, D. 1994a. Estimation of the effective self-diffusion tensor from the NMR spin echo. *J. Magn. Reson.* **103:** 247–254.

Basser, P., Mattiello, J., and LeBihan, D. 1994b. MR diffusion tensor spectroscopy and imaging. *Biophys. J.* **66:** 259–267.

Basser, P., and Pierpaoli, C. 1996. Microstructural and physiological features of tissues elucidated by quantitative-diffusion-tensor MRI. *J. Magn. Reson.* **111:** 209–219.

Basser, P. J. 1998. Fiber-tractography via diffusion tensor MRI (DT-MRI). In *VIth ISMRM, Sydney, AU,* p. 1226.

Besag, J. 1986. On the statistical analysis of dirty pictures. *J. R. Stat. Soc., Ser. B (Methodological)* **48**(3): 259–302.

Bürgel, U., Schormann, T., Schleicher, A., and Zilles, K. 1999. Mapping of histologically identified long fiber tracts in human cerebral hemispheres to the MRI volume of a reference brain: Position and spatial variability of the optic radiation. *NeuroImage* **10:** 489–499.

Chaikin, P., and Lubensky, T. 1995. *Principles of Condensed Matter Physics,* Cambridge, University Press.

Conturo, T. E., Lori, N. F., Cull, T. S., Akbudak, E., Snyder, A. Z., Shimony, J. S., McKinstry, R. C., Burton, H., and Raichle, M. E. 1999. Tracking neuronal fiber pathways in the living human brain. *Proc. Natl. Acad. Sci. USA* **96:** 10422–10427.

Dejerine. 1895. *Anatomie Des Centres Nerveux,* Paris.

Di Virgilio, G., and Clarke, S. 1997. Direct interhemispheric visual input to human speech areas. *Hum. Brain Mapp.* **5:** 347–354.

Filipek, P. A., Kennedy, D. N., Caviness, V. S., Rossnick, S. L., Spraggins, T. A., and Starewicz, P. M. 1989. Magnetic resonance imaging-based brain morphometry: Development and application to normal subjects. *Ann. Neurol.* **25:** 61–67.

Geman, S., and Geman, D. 1984. Stochastic relaxation, Gibbs distributions, and the Bayesian restoration of images. *IEEE Trans. Pattern Anal. Machine Intell.* **PAMI-6**(6): 721–741.

Haselgrove, J. C., and Moore, J. R. 1996. Correction for distorsion of echo-planar images used to calculate the apparent diffusion coefficient. *MRM* **36:** 960–964.

Jones, D. K., Simmons, A., Williams, S. C. R., and Horsfield, M. A. 1999. Non-invasive assessment of axonal fiber connectivity in the human brain via diffusion tensor MRI. *Magn. Reson. Med.* **42:** 37–41.

Le Bihan, D. 1995. *Diffusion and Perfusion Magnetic Resonance Imaging,* Chapt. A-2-IV, pp. 50–57, Raven Press, New York.

LeBihan, D. 1991. Molecular diffusion nuclear magnetic resonance imaging. *Magn. Reson. Q* **7**(1): 1–30.

Makris, N., Worth, A. J., Sorensen, A. G., Papadimitriou, G. M., Wu, O., Reese, T. G., Wedeen, V. J., Davis, T. L., Stakes, J. W., Caviness, V. S., *et al.* 1997. Morphometry of in vivo human white matter association pathways with diffusion-weighted magnetic resonance imaging. *Ann. Neurol.* **42**(6): 951–962.

Makris, N., Meyer, J. W., Bates, J. F., Yeterian, E. H., Kennedy, D. N., and Caviness, V. S. 1999. MRI-based topographic parcellation of human brain cerebral white matter and nuclei. 2. Rationale and applications with systematics of cerebral connectivity. *Neuroimage* **9:** 18–45.

Mangin, J.-F., Coulon, O., and Frouin, V. 1998. Robust brain segmentation using histogram scale-space analysis and mathematical morphology. In *MICCAI'98, MIT, LNCS-1496,* pp. 1230–1241, Springer-Verlag.

Mangin, J.-F., Frouin, V., Bloch, I., Regis, J., and Lopez-Krahe, J. 1995. From 3D magnetic resonance images to structural representations of the cortex topography using topology preserving deformations. *J. Math. Imag. Vision* **5**(4): 297–318.

Meer, P., Mintz, D., Rosenfeld, A., and Kim, D. Y. 1991. Robust regression methods for computer vision: A review. *Int. J. Comput. Vision* **6:** 59–70.

Meyer, J. W., Makris, N., Bates, J. F., Caviness, V. S., and Kennedy, D. N. 1999. MRI-based topographic parcellation of human brain cerebral white matter. 1. Technical foundations. *NeuroImage* **9:** 1–17.

Molnár, Z. 1998. *Development of Thalamocortical Connections,* Springer Verlag.

Mori, S., Crain, B., Chacko, V. P., and van Zijl, P. C. M. 1999. Three dimensional tracking of axonal projections in the brain by magnetic resonance imaging. *Ann. Neurol.* **45:** 265–269.

Pautler, R. G., Silva, A. C., and Koretsky, A. P. 1998. *In vivo* neuronal tract tracing using manganese-enhanced magnetic resonance imaging. *MRM* **40:** 740–748.

Pierpaoli, C., and Basser, P. J. 1996. Toward a quantitative assessment of diffusion anisotropy. *Magn. Reson. Med.* **36:** 893–906.

Pierpaoli, C., Jezzard, P., Basser, P. J., Barnett, A., and DiChiro, G. 1996. Diffusion tensor MR imaging of the human brain. *Radiology* **201:** 637–648.

Poupon, C., Clark, C. A., Frouin, V., LeBihan, D., Bloch, I., and Mangin, J.-F. 1999a. Inferring the brain connectivity from MR diffusion tensor data. In *MICCAI'99, Cambridge, UK, LNCS-1679,* pp. 453–462, Springer-Verlag.

Poupon, C. 1999b. Détection des faisceaux de fibres de la substance blanche pour l'étude de la connectivité anatomique cérébrale, PhD Thesis, ENST Paris.

Poupon, C., Mangin, J.-F., Frouin, V., Régis, J., Poupon, F., Pachot-Clouard, M., LeBihan, D., and Bloch, I. 1998a. Regularization of MR diffusion tensor maps for tracking brain white matter bundles. In *MICCAI'98, MIT, LNCS-1496,* pp. 489–498, Springer-Verlag.

Poupon, C., Mangin, J.-F., Pachot-Clouard, M., Poupon, F., Régis, J., Frouin, V., Bloch, I., and LeBihan, D. 1998b. Tracking fiber bundles in diffusion tensor images. In *NeuroImage,* Vol. 7, No. 4, p. S701.

Pribam, K., and MacLean, P. 1953. Neuronographic analysis of medial and basal cerebral cortex. *J. Neurophysiol.* **16:** 324–340.

Rye, D. B. 1999. Tracking neural pathways with MRI. *Trends NeuroSci.* **22**(9): 373–374.

Tikhonov, A. N., and Arsenin, V. Y. 1977. *Solution of Ill-Posed Problems,* Winston, New York.

Tuch, D. S., Weisskoff, R. M., Belliveau, J. W., and Wedeen, V. J. 1999. High angular resolution diffusion imaging of the human brain. In *VIIth ISMRM,* Philadelphia, PA.

Turner, B., Mishkin, M., and Knapp, M. 1980. Organization of the amygdalopetal projections from modality-specific cortical association areas in the monkey. *Neurology* **191:** 515–543.

Wells, W. M., III, Viola, P. A., Atsumi, H., Najajima, S., and Kikinis, R. 1997. Multi-modal volume registration by maximization of mutual information. *Med. Image Anal.* **1**(1): 35–51.

Westin, C.-F., Maier, S., Khidir, B., Everett, P., Jolesz, F. A., and Kikinis, R. 1999. Image processing for diffusion tensor magnetic resonance imaging. In *MICCAI'99, Cambridge, UK, LNCS-1679,* pp. 441–452, Springer-Verlag.

Whitlock, D. G., and Nauta, W. J. H. 1956. Subcortical projections from temporal neocortex in Macaca mulatta. *J. Comp. Neurol.* **106:** 183–212.

Williams, T. H., Gluhbegovic, N., and Jew, J. Y. 1997. *The Human Brain: Dissections of the Real Brain,* Virtual Hospital, University of Iowa, http://www.vh.org/Providers/Textbooks/BrainAnatomy.

Young, M., Scannell, J., and Burns, G. 1995. *The Analysis of Cortical Connectivity,* Neuroscience Intelligence Unit, Springer Verlag.

Xu, R., van Zijl, C. M., Crain, B. J., Solaiyapppan, M., and Mori, S. 1999. *In vivo* three-dimensional reconstruction of rat brain axonal projections by diffusion tensor imaging. *Magn. Reson. Med.* **42:** 1123–1127.